Int. J. Nano Dimens., 9 (4): 421-434, Autumn 2018

ORIGINAL ARTICLE

Electronic structures and stabilities of endohedral metallofullerenes TM@C34 using DFT approach

Shimaa. Abdel Halim*

Department of Chemistry, Faculty of Education, Ain Shams University, Roxy 11711, Cairo, Egypt

Received 18 March 2018; revised 14 June 2018; accepted 29 July 2018; available online 30 July 2018

Abstract

Theoretical study of the electronic structure using, Density Functional Theory (DFT) calculations at the B3PW91/6-31G (d) level of theory have been employed to the TM@C_{34} (TM =Ti, V, Cr, Mn, Fe, Co, Ni, and Cu) in order to investigate the geometries, electronic structures, binding energies, linear polarizability $\langle\Delta\alpha\rangle$, first order hyperpolarizability $\langle\beta\rangle$, natural bonding orbital (NBO), was studied based on the "C34" fullerene. The results found that the most stable structure is e(C_2). Minimal energy structures of each endohedral metallofullerene were obtained. Hybridizations were found between the Ti, V, Cr, Fe, Co, and Ni, 3d valence orbitals and the "C34" cage orbitals, while none was found between the Mn and Cu orbitals and the "C34" cage orbitals. These findings were obtained with the preferential position of the metal atom inside the fullerene cage, i.e. these results are found suitable for the metal Mn and Cu orbitals present inside the fullerene cage. Natural bonding orbital (NBO), shows that the charges always transfer from the TM atoms to the "C34" cage. In going from isolated TM atom to TM@C_{34}, the occupation of the 4s orbital is strongly reduced. The introduction to TM to the empty "C34" leads to more active NLO performance. The TM@C_{34} (TM =Ti, V, Cr, Mn, Fe, Co, Ni, and Cu) interactions are characterized in terms of several theoretical parameters such as density of states (DOS), molecular electrostatic potentials (MEPs), non-linear optical (NLO) properties and electrophilicity and thermodynamic properties were also performed at B3PW91/6-31G (d) level of theory.

Keywords: *"C34"; DFT Theoretical Investigation; Endohedral Metallofullerene; NLO and NBO Analysis; Structure; Stability; Thermodynamic Properties*

How to cite this article

Abdel Halim S. Electronic structures and stabilities of endohedral metallofullerenes TM@C34 using DFT approach. Int. J. Nano Dimens., 2018; 9 (4): 421-434.

INTRODUCTION

Fullerene related materials have attracted attention because of their unique physical and chemical properties. [1] Fullerenes as cage compounds built exclusively from carbon atoms and their metal-containing forms known as metallofullerenes were for the first time observed in the gas phase [2–6]. The unique spherically shaped cage of "C60" fullerene contains empty space that is large enough to incorporate atoms or molecules inside it [5]. Endohedral metallofullerenes having a single metal atom inside the spherical carbon cage are of interest as new molecules or materials with novel properties such as in designing electronic devices, super fibers, catalytic materials, etc., electrical conductance, magnetism, Ferro electricity, nonlinear optical properties, etc., which are expected to differ much from those of empty fullerenes[6]. Moreover, these properties have also made them prominent species in nanotechnology and bio-medicine [2–6]. Experimentally, although carbon clusters of "C70" are produced in the laser-vaporization process, except for "C60" and "C70", it is still difficult to isolate large quantities of the smaller fullerenes for structural determination. On the other hand, existing theoretical studies can be grouped into two categories are the in- and out-side of cage for TM. In the geometric approach, educated guesses based on mostly symmetry considerations were used to construct plausible topological networks, [7–12]. The topological networks of the fullerenes are constructed by symmetry considerations and by the leapfrog procedure [8–13]. Experiments suggest that fullerenes which incorporate alkali metals posses catalytic properties. Enyashin *et al.* [14] analyzed the electronic structures and

* Corresponding Author Email: *Shimaaquantum@ymail.com*

stability of the crystalline modifications of ''C28'' and Zn@C_{28} using a cluster model. From the point of view of theory, there are several abinitio calculations involving endohedral Li@C_{20} [15] using the density functional nonequilibrium Green's function method, and found that the equilibrium conductance of Li@C_{20} becomes larger than that of the empty ''C20'' molecule. Chen *et al.*. [16] investigated the stabilities and molecular structures of noble gas atoms (i.e. He, Ne, Ar, and Kr) inside the ''C32'' cage. Also Garg *et al.* [17] studied the magnetic properties of 3d transition metals (TM) encapsulated in smaller fullerenes ranging from ''C20'' to ''C36'' by spin polarized density functional theory. In addition to Wu *et al.* [18] has been systematically investigated the structure, electronic property, and infrared spectroscopy of endohedral metallofullerenes TM@C_{20} (TM =Ce and Gd) with the aid of the hybrid DFT-B3LYP functional, and found that the endohedral Metallofullerene Gd@ C_{20} has the high-thermodynamic stability. Moreover the large empty space inside fullerene molecule may be used as storage materials with high capacity and stability. The storage of hydrogen in fullerene has attracted much experimental and theoretical interest, to use in fuel cells for power generation [19]. In the present work we have studied the stability, geometries, binding energies per atom of six fullerene isomers of ''C34'' at DFT/B3PW91 and investigations of endohedral metallofullerenes TM@C_{34} (TM =Ti, V, Cr, Mn, Fe, Co, Ni, and Cu) to predict their stabilities and electronic properties for exploring their potential application. Some properties of these endohedral metallofullerenes have been investigated on the stable structures, including equilibrium structures, relative stabilities, energy gaps (highest occupied molecular orbital [HOMO]–lowest unoccupied molecular orbital [LUMO]), dissociation energy, charge transfers, Natural charges and natural electron configurations have been performed with the Natural Bond Orbital analysis (NBO),density of states (DOS), molecular electrostatic potentials (MEP), and non-linear optical (NLO)properties. Formation energy (ε), ionization potential (I), electron affinity (A), chemical hardness (η), electronegativity (χ), electrophilicity (ω) and thermodynamic properties were investigated on TM@C_{34} (TM =Ti).

Computational details

All the DFT calculations have been performed with the Gaussian 09W (version A.02) software package [20]. The definition for "B3PW91" method is Becke's three-parameter (B3) hybrid exchanges functional [21] with the correlation functional of Perdew and Wang (PW91) [22]. Su, K. H.*et al.* [23,24] shown that B3PW91 method can reproduce the equilibrium structures systematically better than the other methods, such as DFT at BPW91 and B3LYP levels of theory, second order Møller–Plesset perturbation theory (MP2), and quadratic configuration interaction at QCISD and QCISD(T) levels. We considered $3d^24s^2$, $3d^34s^2$, $3d^54s^1$, $3d^54s^2$, $3d^64s^2$, $3d^74s^2$, $3d^84s^2$ and $3d^{10}4s^1$ electronic configurations for Ti, V, Cr, Mn, Fe, Co, Ni and Cu, respectively. Full geometry optimizations and energy calculations of endohedral metallofullerenes TM@C_{34}(TM =Ti, V, Cr, Mn, Fe, Co, Ni, and Cu) were calculated at the B3PW91/6-31G(d) level of theory. All the stationary point geometries were analyzed by evaluating the harmonic vibrational frequencies of the same theoretical level. The figures were generated using the associated Gauss View software. The density of states (DOS) was calculated by using the Gauss Sum 2.2.5 program [25].

RESULTS AND DISCUSSION

Relative stability of C_{34} fullerenes

The total energies (E_{tot}), relative energies (E_{rel}), HOMO–LUMO energy gaps (E.G.), binding energies (BE) and dipole moment (DM) systems of the ''C34'' six isomers are presented in Table 1. The optimized structures of the ''C34'' six isomers are

Table 1. Total energies (E_{tot}), relative energies (E_{rel}), HOMO–LUMO energy gaps (E.G.), Binding energies (BE) and Dipole moment (DM) of six fullerene isomers of ''C_{34}'' calculated at different levels of theory.

Isomer	HF/6-31G(d)		B3PW91/6-31G(d)				
	E_{tot} (Hartrees)	E_{rel} (eV)	E_{tot} (Hartrees)	E_{rel} (eV)	(E. G.) (eV)	BE (eV)	DM (Debye)
a- C_2	-1286.68300877	3.34	-1294.45549860	3.35	1.51	8.57	0.08
b- C_S	-1286.75266795	1.45	-1294.52698622	1.40	1.08	8.81	1.71
c- C_S	-1286.76006422	1.25	-1294.52838845	1.36	1.45	8.81	1.21
d- C_2	-1286.79068719	0.41	-1294.55350150	0.68	1.73	8.83	0.36
e- C_2	-1286.80593488	0.00	-1294.57844214	0.00	1.47	8.85	0.12
f- C_{3V}	-1286.75432890	1.40	-1294.52163142	1.55	1.21	8.80	1.36

obtained using the B3PW91/6-31G(d) level, ''C34'' has six fullerene isomers, i.e., three C_2, two C_s, and one C_{3v} [26], are shown in Fig. 1(a–f). Analysis of data onto Table 1 and Fig. 1(a–f) show that: the e(C_2) isomer has the lowest energy among the six isomers we studied at the two methods HF/6-31G(d) level and B3PW91/6-31G(d) level. At the HF/6-31G(d) level, the stability order for ''C34'' is e(C_2)< d(C_2) <c(C_S) < f(C_{3V}) < b(C_S) < a(C_2). The energy difference between e(C_2) and d(C_2) is 0.41 eV and that between d(C_2) and c(C_S) is 0.83 eV. The energy difference between c(C_S) and f(C_{3V}) is 0.15 eV and that between f(C_{3V}) and b(C_S) is 0.05 eV. The a(C_2) isomer is the least stable. At the B3PW91/6-31G(d) level, the stability order for ''C34'' is e(C_2)< d(C_2) <c(C_S) < b(C_S) < f(C_{3V}) < a(C_2). The relative energies are 0.00,0.68, 1.36, 1.40, 1.55, and 3.35 eV for e(C_2), d(C_2), c(C_S), b(C_S), f(C_{3V}), a(C_2) respectively. They are comparable with the values calculated at HF/6-31G(d)level. At the B3PW91/6-31G(d) level, the order of the binding energies (BE) for ''C34'' is e(C_2)< d(C_2) <c(C_S) < b(C_S) < f(C_{3V}) < a(C_2). The binding energies values per atom are 8.85, 8.83, 8.81, 8.81, 8.80, and 8.57 eV for e(C_2), d(C_2), c(C_S), b(C_S), f(C_{3V}) a(C_2) respectively, this values indicating that the e(C_2) isomer is more stable. Fig. 2, shows the isodensity surface of HOMO and LUMO of the ''C34'' six isomers. The HOMO–LUMO energy gap has been used as an index of kinetic stability for fullerenes [27], which means that a fullerene molecule with a larger HOMO–LUMO gap will be chemically less reactive. The results show that the HOMO–LUMO gap between isomer d(C_2) is the biggest one

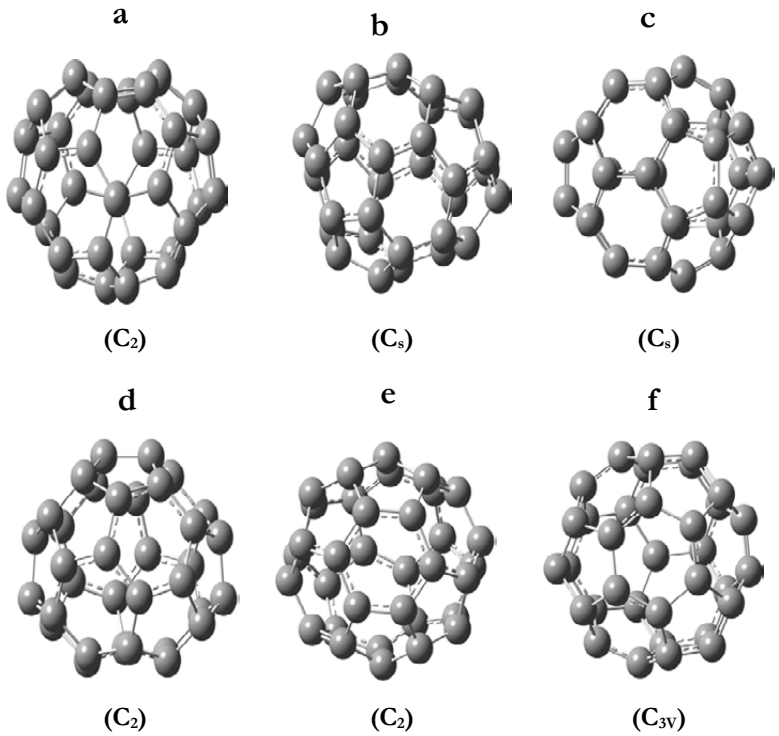

Fig. 1. Optimized geometries of Molecular structures of the six (a-f) ''C34'' isomers.

Table 2. The electronic configuration, orbital diagram, spin multiplicity, and total electronic energy of free TM (TM =Ti, V, Cr, Mn, Fe, Co, Ni, and Cu) in the low-spin state at the B3PW91/6-31G(d) level of theory.

Electronic configuration		Orbital diagram	Spin multiplicity	Energy E_{au}
^{22}Ti[Ar]3d^{2}4s^2	3d^4	↓↑↓↑	singlet	-849.16013
^{23}V[Ar]3d^{3}4s^2	3d^5	↓↑↓↑↑	doublet	-943.66772
^{24}Cr[Ar]3d^{5}4s^1	3d^6	↓↑↑↑↑↑	quintet	-1044.0589
^{25}Mn[Ar]3d^{5}4s^2	3d^7	↓↑↓↑↑↑↑	quartet	-1150.6057
^{26}Fe[Ar]3d^{6}4s^2	3d^8	↓↑↓↑↓↑↑↑	triplet	-1263.3098
^{27}Co[Ar]3d^{7}4s^2	3d^9	↓↑↓↑↓↑↓↑↑	doublet	-1382.4058
^{28}Ni[Ar]3d^{8}4s^2	3d^{10}	↓↑↓↑↓↑↓↑↓↑	single	-1507.8778
^{29}Cu[Ar]3d^{10}4s^1	3d^{10}4s^1	↓↑↓↑↓↑↓↑↓↑	doublet	-1640.1233

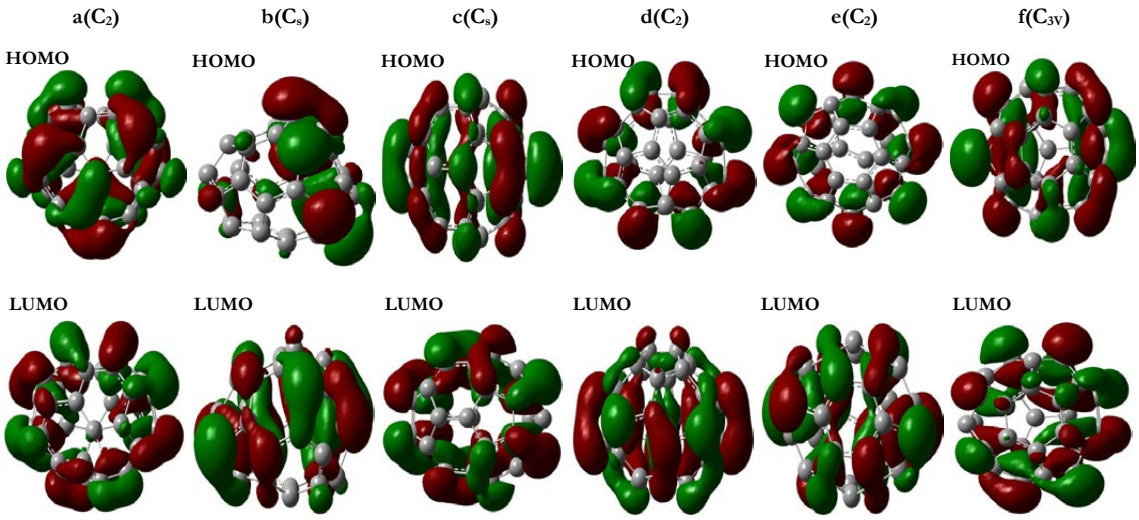

Fig. 2. Frontier orbital isosurface plots (isodensity contours=0.02 a.u.) of the six (a-f) ''C_{34}'' isomers.

Table 3. The average C–C and C=C bond lengths , distance between transition metal and center, the shortest transition metal-carbon bond length (in Å), the cohesive energy (ΔE), the Gibbs energies (ΔG), binding energies (BE), average cage diameter and the zero-point correction energy of TM@C_{34}(TM =Ti, V, Cr, Mn, Fe, Co, Ni, and Cu) at the B3PW91/6-31G(d) level of theory.

Molecule	$C-C$	$C=C$	TM-Center	TM-C	ΔE(eV)	ΔG (eV)	BE (eV)	average cage diameter	ZPE(a.u.)
C_{34}	1.45-1.50	1.39-1.45	----	----	----	----	-300.8	4.84	0.206545
Ti@C_{34}	1.45-1.50	1.39-1.45	0.67	2.06	8.33	4.486	-7.117	0.67	0.227832
V@C_{34}	1.45-1.49	1.40-1.44	0.76	2.02	7.16	4.616	-6.089	0.76	0.206300
Cr@C_{34}	1.45-1.52	1.40-1.45	0.88	1.91	7.32	4.523	-6.058	0.88	0.208080
Mn@C_{34}	1.45-1.50	1.40-1.44	0.20	2.20	5.25	4.814	-4.763	0.20	0.204154
Fe@C_{34}	1.45-1.49	1.41-1.44	0.93	1.84	5.35	4.754	-4.249	0.93	0.205562
Co@C_{34}	1.45-1.50	1.40-1.45	0.61	2.06	3.78	5.111	-3.290	0.61	0.203215
Ni@C_{34}	1.45-1.50	1.39-1.44	0.68	1.95	4.50	4.947	-3.826	0.68	0.203756
Cu@C_{34}	1.45-1.50	1.39-1.44	0.00	2.47	2.82	5.214	-2.529	0.00	0.202107

(1.73 eV) and shows its kinetic stability. The e(C_2) isomer, predicted to have the lowest energy, has a large HOMO–LUMO gap between 1.47 eV in our calculation, indicating that it is kinetically stable.

Optimized equilibrium geometries of endohedral metallofullerenes TM@C_{34}

In this study, we have considered the electronic state for free TM (TM =Ti, V, Cr, Mn, Fe, Co, Ni, and Cu) in the low-spin state at the B3PW91/6-31G(d) levels of theory. In Table 2, the theoretical electronic configuration of TM in the gas phase is given together with the spin multiplicity, spin state, electronic state and total electronic energy. The ''C34'' cage with e(C2) symmetry Fig. 1 is considered the starting cage configuration to investigate the endohedral metallofullerenes TM@C34(TM =Ti, V, Cr, Mn, Fe, Co, Ni, and Cu). The average C–C and C=C bond lengths , distance between transition metal and center, the shortest transition metal-carbon bond length (in Å) are given in Table 3. For Mn@C_{34}, the stable structure found with the metal atom located at off-center of the ''C34'' cage not in the middle of the carbon cage according to the data in Table 3 is 0.20 Å, while Cu@C_{34}, the stable structure found with the metal atom located at middle -center of the ''C34'' cage and according to the data in Table 3 is 0.00 Å for Cu@C_{34}. In the case of Ti@C_{34}, V@C_{34}, Cr@C_{34}, Fe@C_{34}, Co@C_{34}, and Ni@C_{34}, the stable structure found with the metal atom moved from the center of one pentagonal face and then linked to this face.

''C34'' has an average diameter of 4.84 Å and the binding energy per atom is -300.8 eV with average C–C and C=C bond lengths 1.45-1.50 Å and 1.39-1.45 Å respectively. The optimized structures of the endohedral metallofullerenes TM@C34(TM =Ti, V, Cr, Mn, Fe, Co, Ni, and Cu) are shown in Fig. 3. As a result of TM substitution inside ''C34''

cage, the average diameter shows a slight increase in a maximum value of 0.93 Å for Fe@C34. The average C–C and C=C bond lengths of TM@C34 complexes lie in the range 1.45-1.52 Å (see Table 3). The binding energy per atom is higher for Ti@C34 ,and V@C34, -7.117 eV and -6.089 eV for Ti and V respectively and decreasing value for other TMs. Further, the interaction between the fullerene cage and TMs along with the stabilities of TM@Cn complexes is described by evaluating their cohesive energies. We define the cohesive energy of TM@Cn complexes as follows:

$$\Delta E = E(\mathrm{C}_n) + E(\mathrm{TM}) - E_{\mathrm{Total}}\,(\mathrm{TM@C}_n) \qquad (1)$$

Where E_{Total} (TM@C_n), E(C_n) and E(TM)) are the total energies of the endohedral complex, isolated fullerene and TM atoms, respectively. The cohesive energies ''ΔE'' calculated using eqn (1) are presented in Table 3. The positive values of ΔE indicate the greater stability of TMs inside fullerene cage and are likely to be formed experimentally. The negative values of ΔE indicate that the corresponding TM encapsulated in the fullerene cage is unstable or less stable and have not been experimentally observed. The cohesive energies tabulated in Table 3 shows positive cohesive energies for all the TMs leading to the fact that they all form stable complexes about ''C34''. The stability order for TM@C_{34} is (TM= Ti< Cr < V< Fe <Mn < Ni < Co< Cu). On the basis of reaction Gibbs energies, the thermodynamic stability of TM@C34 in context of this reaction can be assessed. The negative values of ΔG (Gibbs energies), indicate the greater stability of TMs thermodynamically and the positive values of ΔG, indicate the smallest stability of TMs thermodynamically. The Gibbs energies tabulated in Table 3 shows positive values Gibbs energies for all the TMs . The stability order by smallest positive values of ΔG for TM@C_{34} is (TM= Ti< Cr < V< Fe <Mn < Ni < Co< Cu). As shown in Table 3, all encapsulation processes, is endothermic; this is likely due to swelling for the ''C34'' cage upon encapsulation of TM, these present change in enthalpy data of Ti-metal as example for the positive value of enthalpy data indicating that "endothermic" in Table 7. Here, all eight TM@C34 are at the local minima because they have all real frequencies. The order of the zero-point correction energy for TM@C34 has the same order of stability order.

Frontier orbital analyses, energy gaps

The highest occupied molecular orbital (HOMO) and the lowest unoccupied molecular orbital (LUMO) are frequently referred to as frontier molecular orbital's (FMOs). Fig. 4 shows the frontier orbital surfaces (0.02 eV/a.u.) of HOMO and LUMO of empty ''C34'' and TM@C_{34}(TM =Ti, V, Cr, Mn, Fe, Co, Ni, and Cu). From the frontier

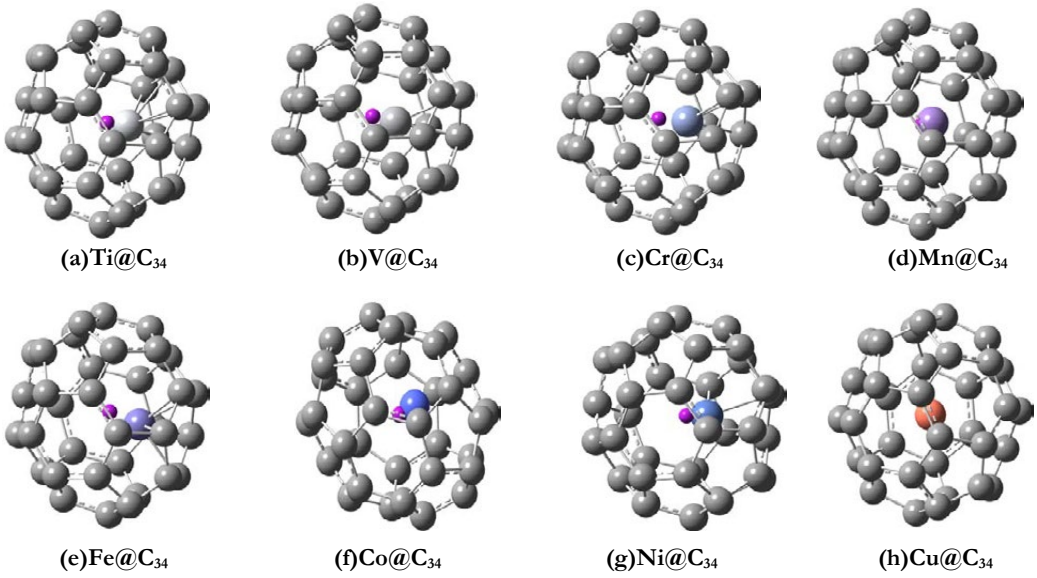

Fig. 3. Optimized geometries (a-h) of Endohedral Metallofullerenes TM@C_{34}(TM=Ti, V, Cr, Mn, Fe, Co, Ni, and Cu).

The "red atom" is located in the middle of the fullerene cage, and it does not resemble an additional atom so; I put it in cage to determine the average cage diameter length of all TM in fullerene cage complex (TM@C_{34}).

molecular orbitals illustrated, in Fig. 4 we could see that there is no hybridization between Mn and Cu atomic orbitals and the ''C34'' cage orbitals. The HOMO and LUMO of TM@C_{34} (TM =Ti, V, Cr, Fe, Co, and Ni) shows obviously mixing between the orbitals of the ''C34'' cage and 3d orbitals of the transition metal atoms. The orbital hybridization between the guest transition metal atoms and fullerene cage is a common characteristic in metallofullerenes [28 – 32].

The energy gaps between the empty ''C34'' cage and TM@C_{34} (TM =Ti, V, Cr, Mn, Fe, Co, Ni, and Cu) are given in Table 4. The HOMO–LUMO gap between ''C34'' is 1.47 eV which is calculated from HOMO (-5.53 eV) and LUMO (-4.06 eV). When the endohedral metallofullerenes TM@C_{34} (TM =Ti, V, Fe, Ni, and Cu), both of the HOMO and LUMO orbital energies are higher by (0.26,0.15,0.19,0.23,0.05) and (0.58,0.55,0.39,0.27,0.31) eV, respectively; this leads to the slightly large HOMO–LUMO gap (1.79,1.89,1.67,1.51 and 1.73 eV) respectively.

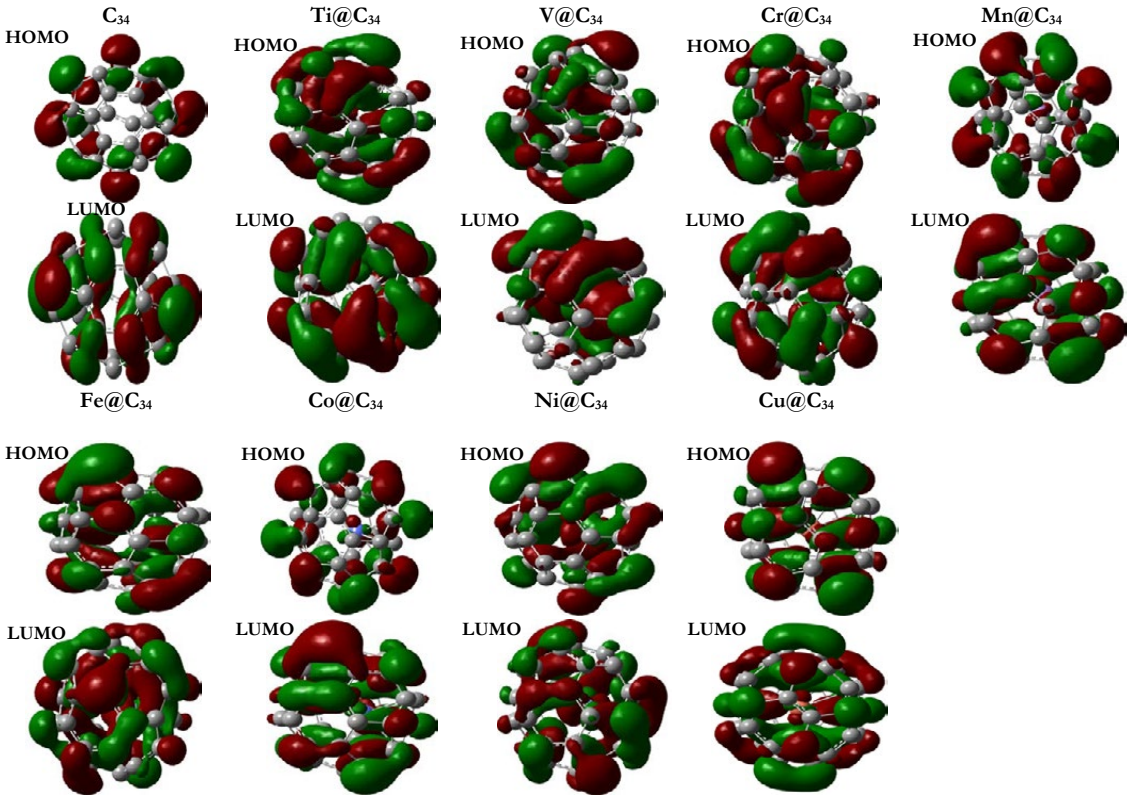

Fig. 4. Frontier orbital isosurface plots (isodensity contours=0.02 a.u.) of Endohedral Metallofullerenes TM@C_{34}(TM=Ti, V, Cr, Mn, Fe, Co, Ni, and Cu).

Table 4. Frontier orbital energy levels (HOMO and LUMO) and energy gaps (E.G.), natural charge population, and natural electron configuration of the most stable TM@C_{34}(TM =Ti, V, Cr, Mn, Fe, Co, Ni, and Cu) calculated at the B3PW91/6-31G(d) level of theory.

Molecule	HOMO(eV)	LUMO(eV)	(E.G.)(eV)	Natural charge on TM atom	Natural electron configuration on TM atom
C34	-5.53	-4.06	1.47	---	---
Ti@C_{34}	-5.27	-3.48	1.79	0.70	[core]4S$^{(0.01)}$3d$^{(2.66)}$4p$^{(0.37)}$4d$^{(0.01)}$6S$^{(0.26)}$
V@C_{34}	-5.38	-3.49	1.89	0.76	[core]4S$^{(0.21)}$3d$^{(3.66)}$4p$^{(0.36)}$5S$^{(0.01)}$4d$^{(0.01)}$
Cr@C_{34}	-5.20	-3.74	1.46	0.58	[core]4S$^{(0.18)}$3d$^{(4.86)}$4p$^{(0.37)}$5S$^{(0.01)}$4d$^{(0.01)}$
Mn@C_{34}	-5.51	-4.04	1.47	1.06	[core]4S$^{(0.17)}$3d$^{(5.42)}$4p$^{(0.33)}$5S$^{(0.02)}$
Fe@C_{34}	-5.34	-3.67	1.67	0.69	[core]4S$^{(0.14)}$3d$^{(6.83)}$4p$^{(0.32)}$5S$^{(0.01)}$
Co@C_{34}	-5.50	-4.07	1.43	0.90	[core]4S$^{(0.20)}$3d$^{(7.50)}$4p$^{(0.37)}$5S$^{(0.02)}$5p$^{(0.01)}$
Ni@C_{34}	-5.30	-3.79	1.51	0.64	[core]4S$^{(0.20)}$3d$^{(8.74)}$4p$^{(0.39)}$5S$^{(0.02)}$5p$^{(0.01)}$
Cu@C_{34}	-5.48	-3.75	1.73	0.38	[core]4S$^{(0.29)}$3d$^{(9.74)}$4p$^{(0.54)}$5S$^{(0.04)}$5p$^{(0.01)}$

The energy gaps between $Mn@C_{34}$, is the same as that of the empty ''C34'' cage (1.47 eV). It was confirmed that the Mn and Cu atom and the ''C34'' cage are not covalent. A large HOMO–LUMO gap can be used as a simple indicator of high kinetic stability and low chemical reactivity [33]. Thus, it is indicated that the modified ''C34'' derivatives by Ti, V, Mn, Fe, Ni, and Cu atoms increase their kinetic stabilities. The energy gaps between $Cr@C_{34}$ and $Co@C_{34}$ are smaller than that of the empty ''C34'' cage, being 1.46, and 1.43 eV, respectively. Interestingly the $Fe@C_{34}$ and $Cr@C_{34}$ possesses the larger dipole moments, being 2.93 and 2.42 D, respectively.

Natural population analysis

Natural bond orbital (NBO) has an important role in interaction in complex, specially charge to transfer. The natural charges and natural electron configurations on TM atoms in the most stable $TM@C_{34}$ (TM = Ti, V, Cr, Mn, Fe, Co, Ni, and Cu) are listed in Table 4. From this table, we can see that the charge transfer from the TM atoms to the ''C34'' cage, so we can consider the fullerene ''C34'' cage acts an electron acceptor. Also, from our calculation results Table 4 we show that no matter whether the valence electrons of the TM atoms are 4–11, the charge transfer is less than 2e. The isolated Ti atom has the following natural electron configurations $4s^2 3d^2$, but in Ti $@C_{34}$ the Ti atom has the following electron configurations: $4S^{0.01}3d^{2.66}4p^{0.37}4d^{0.01}6S^{0.26}$. In going from isolated Ti atom to $Ti@C_{34}$, the occupation of the 4s orbitals is strongly reduced. The Ti atom forms an ionic bond between the ''C34'' cage, and transfers only 0.70e to the cage. The charge is donated by the 4s orbitals of Ti atom and transfers 0.66e to its 3d orbitals. Similarly, the V, Mn, Fe, Co, and Ni atom transfer 0.76e, 1.06e, 0.69e, 0.90e, and 0.64e to the ''C34'' cage, respectively. These results indicated that the 3d orbitals are the main valence orbitals. For $Cr@C_{34}$ and $Cu@C_{34}$ the situation is different, in $Cr@C_{34}$ the electron configurations on Cr atom is $4S^{0.18}3d^{4.86}4p^{0.37}5S^{0.01}4d^{0.01}$. When compared with the $4s^1 3d^5$ configurations of isolated Cr atom, it was found that the Cr atom transfers 0.58e to the ''C34'' cage that charge is donated by the 4s and 3d orbitals of Cr atom. In $Cu@C_{34}$, we found that the Cu atom transfers 0.38e to the ''C34'' cage that charge is donated by the 4s and 3d orbitals of Cu atom.

Density of states and molecular electrostatic potentials

As shown in Table 4, the HOMO–LUMO energy gaps are reduced under the effect of introduced Cr@C34 and Co@C34 and implies that the density of states (DOS) become more abundant near Fermi levels. In solid state and condensed matter physics, the density of states of a system describes the number of states per interval of energy at each energy level that are available to be occupied by electrons. A high DOS at a specific energy level means that there are many states available for occupation. The calculated DOS are presented in Fig. 5 to clarify the effects of endohedral metallofullerenes TM@C34(TM =Ti, V, Cr, Mn, Fe, Co, Ni, and Cu). As shown, DOS become more abundant near Fermi levels in both Cr@C34 and Co@C34, where the overall features of DOS change, and deep vales develop on both sides nearby Fermi levels.

Molecular electrostatic potential (MEP)

The MEP contours or surfaces have been established extensively as a guide to the interpretation and prediction of molecular behavior [34]. It has been shown to be a useful tool for studying both electrophilic and nucleophilic processes, in particular the ''recognition'' of one molecule by another [35]. MEPs are either negative, low potentials that are characterized by an abundance of electrons and reactive with electrophiles, or positive, high potentials that are characterized by an absence of electrons and reactive with nucleophiles. We denote the former by a deep red color, and the later with a deep blue color. The molecular electrostatic potential surfaces (MEP) of empty ''C34'' and endohedral metallofullerenes $TM@C_{34}$(TM =Ti, V, Cr, Mn, Fe, Co, Ni, and Cu) are given in Fig. 6. The electron color scheme for the MEP surface is as follows: (deep red) low MEPs for electron rich, (the negative charge); (deep blue) high potentials for deficient, (the positive charge); respectively.

As shown, the intensities of the positive and negative MEP surfaces are more affected by endohedral metallofullerenes than the empty ''C34''. For both $Cr@C_{34}$ and $Co@C_{34}$, the negative (deep red) low MEPs that are characterized by an abundance of electrons and reactive with electrophiles predominate the region of the ''C34'' and extend to the Cr and Co. Simultaneously, the positive (deep blue) high potentials are significantly

reduced in these regions. It is therefore concluded that the TM regions of both Cr@C_{34} and Co@ C_{34} are more readily available for electrophilic processes, while the ''C34'' regions are more readily available for nucleophilic processes. For both Mn@C_{34} and Cu@C_{34}, we notice that Mn and Cu are located at off-center of the ''C34'' cage and the MEP distributions for them are too similar to the empty ''C34'' cage.

Non-linear effects

The non linear optical (NLO) properties, such as polarization and hyper- polarization characterize the response of a system in an applied electric field and determine the strength of molecular interactions as well as the cross-sections of different scattering and collision processes. The electronic dipole moment, molecular polarization, anisotropy of polarization and first hyper-polarization of the empty ''C34'' and TM@C_{34}(TM =Ti, V, Cr, Mn, Fe, Co, Ni, and Cu) are investigated. The higher values of molecular polarization and dipole moments are important for more active NLO performance. The NLO phenomena occur to sufficiently intense fields. As the applied field strength increases, the polarization response to

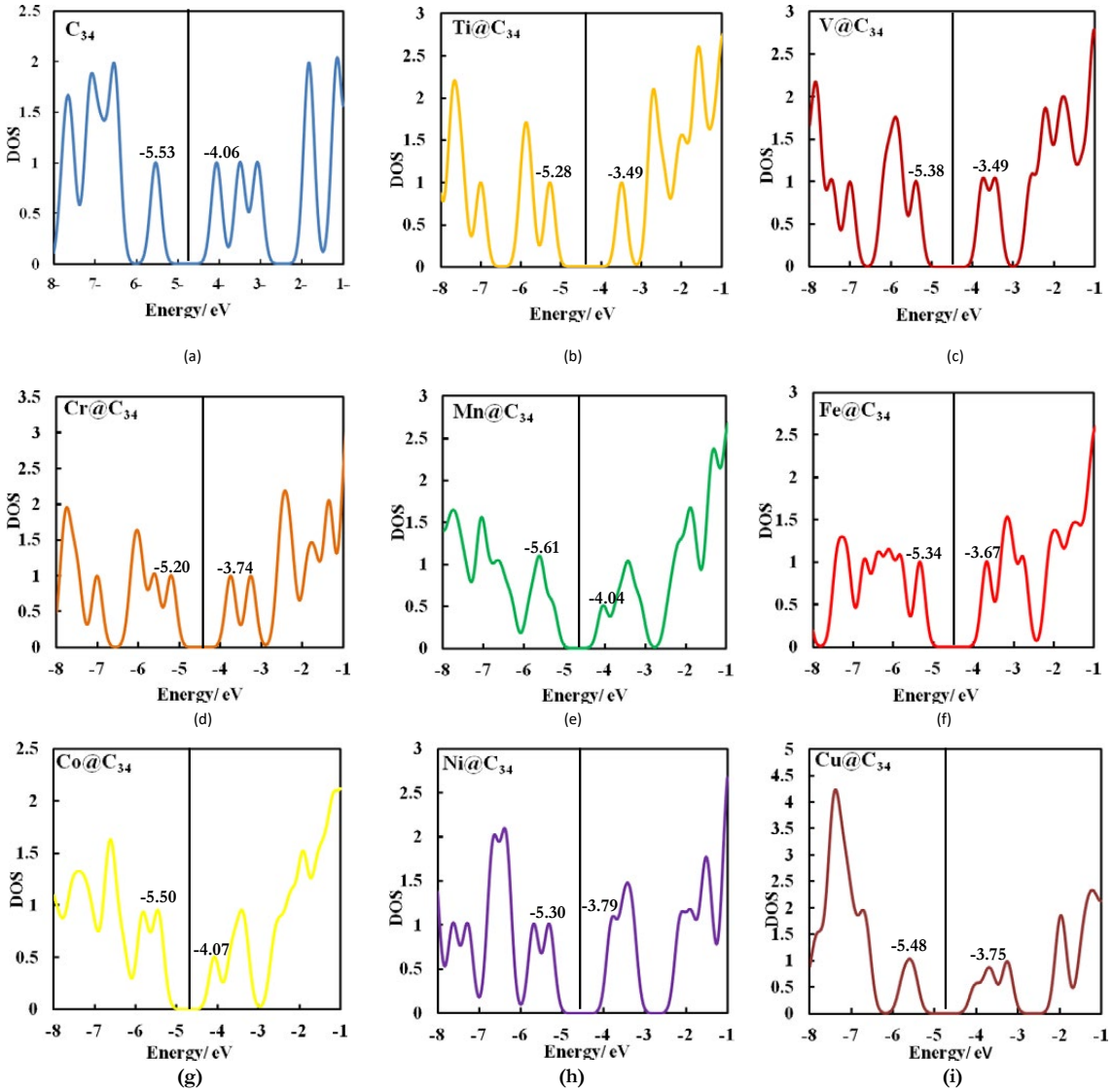

Fig. 5. HOMOs, LUMOs and density of states (DOS) (a-i) of the Endohedral Metallofullerenes TM@C_{34}(TM=Ti, V, Cr, Mn, Fe, Co, Ni, and Cu). Vertical lines Fermi levels.

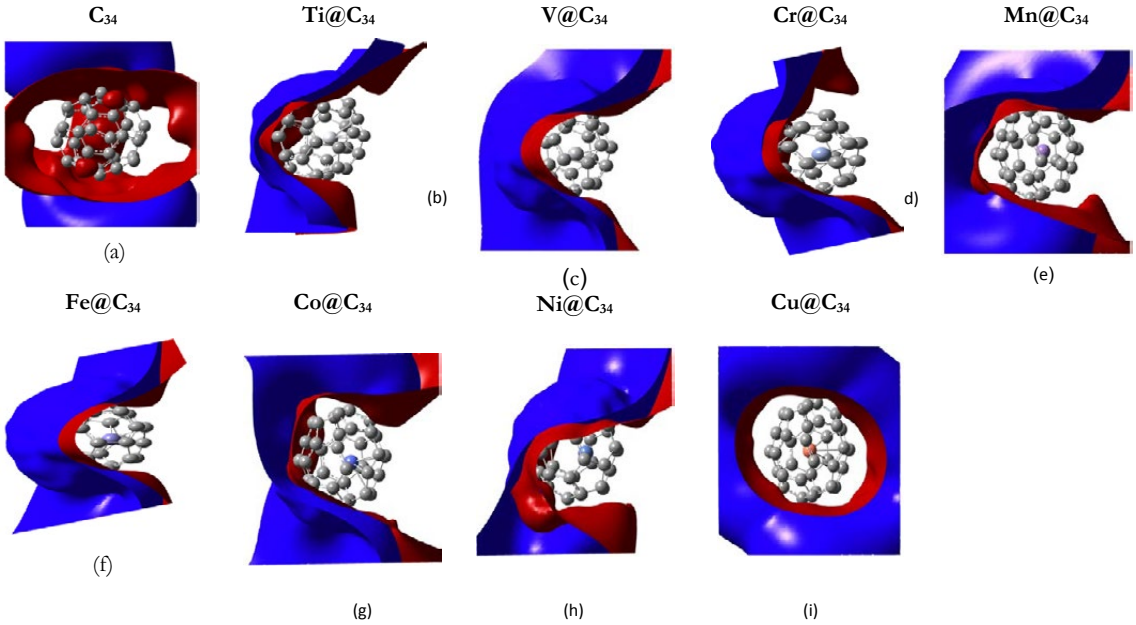

Fig. 6. Side view of molecular electrostatic potential MEP surfaces contours (a-i) of the Endohedral Metallofullerenes TM@ C_{34}(TM=Ti, V, Cr, Mn, Fe, Co, Ni, and Cu).

The electron color scheme for the MEP surface is as follows: (deep red) low MEPs for electron rich, (the negative charge); (deep blue) high potentials for deficient, (the positive charge); respectively.

the medium is no longer linear and the induced polarization (P) becomes a function of the applied field [36].

$$P = \chi^{(1)}E + \chi^{(2)}E^2 + \chi^{(3)}E^3 + \cdots \quad (2)$$

where the $\chi^{(2)}$ and $\chi^{(2)}$ coefficients represent the second and third-order susceptibilities of the medium, respectively. At the molecular level, Equation (2) is expressed as [37]

$$P = \sum_{j} \alpha_{ij} E + \sum_{j<k} \beta_{ijK} E^2 + \sum_{j<k<l} \gamma_{ijKl} E^3 + \cdots \quad (3)$$

Where α_{ij} = polarization, β_{ijK}=first hyper-polarization (second-order effects), γ_{ijKl}=second hyper- polarization (third-order effects), and i,j,K,l correspond to the molecular coordinates.

The average linear polarization (α_{tot}) and the anisotropy of the polarization ($\Delta\alpha$) are calculated as follows [38]

$$\alpha_{tot} = 1/3\ (\alpha_{xx} + \alpha_{yy} + \alpha_{zz}), \quad (4)$$

$$\Delta\alpha = ((\alpha_{xx} - \alpha_{yy})^2 + (\alpha_{yy} - \alpha_{zz})^2 + (\alpha_{zz} - \alpha_{xx})^2/2)^{1/2}, \quad (5)$$

The tensor of the static first-order hyper-polarization is a result of the third derivative of the energy with respect to the electric field components. The second order polarization or first hyper-polarization (β_{tot}) is calculated as follows:

$$\langle\beta\rangle = (\beta^2_x + \beta^2_y + \beta^2_z)^{1/2}, \quad (6)$$

Where

$$\beta_x = \beta_{xxx} + \beta_{xyy} + \beta_{xzz},$$
$$\beta_y = \beta_{yyy} + \beta_{xxy} + \beta_{yzz},$$
$$\beta_z = \beta_{zzz} + \beta_{xxz} + \beta_{yyz}.$$

The total dipole moment μ_{tot} can be calculated by using the following equation:

$$\mu_{tot} = (\mu^2_x + \mu^2_y + \mu^2_z)^{1/2} \quad (7)$$

Where μ_i (i =x,y,z) is the electronic dipole moment.

The hyper- polarization, dipole moment and polarization for empty ''C34'' cage and TM@ C_{34} (TM =Ti, V, Fe, Ni, and Cu) are presented in Table 5. Several facts emerge from Table 5: (1) the larger polarization α_{tot} is assigned to Mn@C_{34} and

Table 5. Polarizabilities (α), hyperpolarizabilities (β), and dipole moments (μ) of the empty ''C_{34}'' and TM@C_{34}(TM =Ti, V, Cr, Mn, Fe, Co, Ni, and Cu), calculated at the B3PW91/6-31G (d) level of theory.

	α_{XX}	α_{XY}	α_{YY}	α_{ZZ}	α_{YZ}	α_{XZ}	α_{tot}	$\Delta\alpha$	μ_x	μ_y	μ_z	μ_{tot}
C_{34}	307.257	2.133	261.969	0.026	0.013	241.884	270.4	58.12	0.0162	0.0011	-0.1541	0.155
Ti@C_{34}	304.314	-1.734	268.939	-0.854	-3.352	246.567	273.3	50.87	-0.2931	-0.7782	0.1721	0.849
V@C_{34}	306.437	-0.936	276.138	0.132	4.036	247.693	276.8	51.39	0.1248	-0.5953	0.2767	0.668
Cr@C_{34}	308.100	-3.855	269.612	-2.521	-4.055	248.885	275.5	53.12	-0.0851	-0.9431	-0.0927	0.951
Mn@C_{34}	323.855	0.244	273.286	-0.577	-0.223	251.102	282.7	64.59	-0.0728	-0.2400	-0.0805	0.263
Fe@C_{34}	300.012	-3.804	271.764	0.764	-2.198	249.035	273.6	44.90	-0.5181	-0.9654	-0.2811	1.131
Co@C_{34}	319.290	0.198	273.049	0.934	-1.267	251.885	281.4	59.77	0.0228	-0.3535	-0.1013	0.368
Ni@C_{34}	306.560	1.758	272.874	-1.817	-0.261	249.743	276.4	49.72	-0.3184	-0.6495	-0.2050	0.752
Cu@C_{34}	317.632	-2.814	271.833	-0.043	-0.017	247.435	279.0	61.92	-0.0007	0.0123	-0.0752	0.076

	β_{xxx}	β_{xxy}	β_{xyy}	β_{yyy}	β_{xxz}	β_{xyz}	β_{yyz}	β_{xzz}	β_{yzz}	β_{zzz}	β_{II}	β_{total}
C_{34}	-3.838	-1.415	-0.562	-1.969	70.927	29.716	50.877	-0.612	0.153	-11.40	66.244	110.57
Ti@C_{34}	-193.731	-25.862	-30.475	-207.980	-31.545	37.446	10.863	-72.531	-90.999	7.45	-7.938	440.17
V@C_{34}	-121.387	331.301	-315.244	688.160	33.822	83.779	-37.760	105.530	-75.661	45.61	25.004	1001.06
Cr@C_{34}	-9.051	-125.373	32.607	-273.481	75.479	34.280	29.785	-88.612	-42.301	-23.55	49.026	453.35
Mn@C_{34}	-174.394	15.074	-12.912	4.800	-415.361	11.538	-13.765	-27.140	-32.979	-19.27	-269.037	497.21
Fe@C_{34}	-194.586	-97.750	-29.501	-137.254	-3.638	16.110	51.024	-114.738	-82.441	-55.26	-4.727	464.37
Co@C_{34}	1000.483	169.145	107.679	-36.075	-214.949	27.062	-25.214	72.711	16.433	3.60	-141.937	1213.58
Ni@C_{34}	-202.790	-103.264	-36.734	-86.212	-47.983	15.627	44.360	-60.437	-86.829	-74.87	-47.093	415.31
Cu@C_{34}	-6.507	2.430	-0.588	-0.266	-203.125	12.882	5.664	0.122	0.030	-4.306	-121.060	201.90

dominated by the term α_{xx}. All of the polarization terms are significantly affected by incorporation of TM; (2) the larger resultant dipole moment μ_{tot} is assigned to Fe@C_{34}, and dominated by the term μ_y. The dipole moment components μ_x, μ_y, and μ_z, are significantly affected by incorporation of TM; (3) the larger positive value of the total hyper-polarization term β_{total} is assigned to Co@C_{34} and dominated by the positive termβ_{xxx}. All of the hyper- polarization terms are significantly affected by incorporation of TM. These results indicate that the polarization α, resultant dipole moment μ, and hyper-polarization β distinguish between TM@C_{34} complex and empty ''C34'' cage, where larger values of polarization, hyper- polarization, and dipole moments are assigned to the former. For these systems, the relative NLO activities are in order: Cu@C_{34}> Ni@C_{34}> Ti@C_{34}> Cr@C_{34}> Fe@ C_{34}> Mn@C_{34}> V@C_{34}> Co@C_{34} , indicating that the structural modification by TM atom strengthens the second-order NLO response because the encapsulated atoms induce the localized bonding interactions in the inner surface of cage. There are no available experimental or theoretical values for comparison; however, we hope that all theoretical evidences would provide some chemical insight to characterize these complexes for the sake of their future experimental exploration.

Electrophilicity

The ionization potential *(I)* and electron affinity *(A)* can be calculated from relations 8 and 9:

$$I = E^{+1} - E^{0} \quad (8)$$

$$A = E^{0} - E^{-1} \quad (9)$$

Where *I* and *A* are obtained from the total electronic energies E^{+1}, E^{0} and E^{-1} of the cation, neutral, and anion forms of TM@C_{34} at the neutral geometry, i.e. the optimized geometry of neutral complex TM@C34 E^0 used for calculations of energies of both its cation E^{+1} and anion forms E^{-1} . In DFT, the natural (optimized geometry complex TM@C34) way to approximate electronegativity (χ) [39,40] and chemical hardness *(η)* [41,42] is to evaluate them directly from the calculated *I* and *A* as shown in the following equation (10,11):

$$\chi = -\mu = (I + A)/2 \quad (10)$$

$$\eta = (I - A)/2 \quad (11)$$

The electrophilicity [43–45] *(ω)* is defined as

$$\omega = \mu^2/ 2\eta \quad (12)$$

The Ionization potential*(I/eV)*, electron affinity *(A/eV),* chemical hardness *(η/eV),* electronegativity *(χ / eV),* chemical potential (*μ* / eV) and electrophilicity *(ω/eV)* of TM@C_{34} are collected in Table 6. Chemical hardness (η) can be used as complementary tool to describe the thermodynamic aspects of chemical reactivity. Our computational study shows that the hardness (η) of the complex Co@C_{34} is smaller than that of the complex V@C_{34} indicating a decrease in the rigidity of the Co@C_{34} complex thereby decreasing its stability. A good electrophile will be characterized

by a high value of electrophilicity (ω). It is therefore evident that while the complexs $V@C_{34}$ are better electrophile than $Co@C_{34}$, it is more stable and less reactive than $Co@C_{34}$ complex.

Thermodynamic properties

Vibrational analysis and statistical thermodynamics, the standard thermodynamic functions, the heat capacity ($C^0_{p,m}$), entropy (S^0_m), and enthalpy (H^0_m), for both $TM@C_{34}$ and TM =Ti were obtained at the B3PW91/ 6−31G(d) level and are listed in Table 7. The table shows that the standard heat capacities, entropies, and enthalpies increase at any temperature from 200.00 to 600.00 K, because the intensities of the molecular vibration increase with the increasing temperature. The correlations between these thermodynamic properties and temperatures T are shown in Fig. 7. The correlation equations are as follows:

$$C^0_{p,m,C34} = -9.98222 + 0.24615\ T - 4.38172\times10^{-4}\ T^2;\ (R^2 = 0.99378),\quad (13)$$

$$C^0_{p,m,Ti\text{-}C34} = -8.83333 + 0.25447\ T - 4.59044\times10^{-4}\ T^2;\ (R^2 = 0.99361),\quad (14)$$

$$S^0_{m,C34} = 37.47622 + 0.22856\ T + 0.84529\times10^{-5}\ T^2;\ (R^2=0.99973),\quad (15)$$

$$S^0_{m,Ti\text{-}C34} = 38.12089 + 0.24011\ T - 0.80505\times10^{-4}\ T^2;\ (R^2=0.99978),\quad (16)$$

$$H^0_{m,C34} = 111.22422 - 0.00532\ T + 2.2347\times10^{-4}\ T^2;\ (R^2 = 0.98804),\quad (17)$$

$$H^0_{m,Ti\text{-}C34} = 111.51378 - 0.00551\ T + 2.3134\times10^{-4}\ T^2;\ (R^2 = 0.98838).\quad (18)$$

These equations will be helpful for the further studies for both $TM@C_{34}$ and TM =Ti compounds [46,47].

CONCLUSIONS

In summary, using the *ab initio* and density functional theory (DFT) methods, the author has studied the structure and stability of ''C34'' fullerene isomers and predicted that the e(C_2) isomer is the ground state of ''C34''. In this work, we have performed the theoretical investigations into $TM@C_{34}$ (TM =Ti, V, Cr, Mn, Fe, Co, Ni, and Cu) using the hybrid DFT-B3PW91 functional in conjunction with 6-31G(d) basis sets. For systematically exploring these complexes, some properties were considered, such as relative stabilities E_{HOMO}, E_{LUMO}, energy gap, dissociation energy , natural population analysis, the density of states (DOS), molecular electrostatic potential (MEP) , and nonlinear optical (NLO) properties. We found that the stable structure of $Mn@C_{34}$ and

Table 6. Total energy (E_{total}, a.u), formation energy (ε, eV), ionisation potential (I, eV), electron affinity (A, eV), chemical hardness (η, eV), electronegativity (χ, eV), and electrophilicity (ω, eV) of the $TM@C_{34}$(TM =Ti, V, Cr, Mn, Fe, Co, Ni, and Cu), calculated at the B3PW91/6-31G(d) level of theory.

System	*E*	*ε*	*I*	*A*	*η*	*χ*	*ω*
C_{34}	-1294.5784	-300.8	5.530	4.057	0.736	4.793	7.801
$Ti@C_{34}$	-2144.0001	-7.117	5.277	3.486	0.895	4.381	5.359
$V@C_{34}$	-2238.4699	-6.089	5.383	3.488	0.947	4.435	5.191
$Cr@C_{34}$	-2338.8600	-6.058	5.198	3.744	0.727	4.471	6.874
$Mn@C_{34}$	-2445.3592	-4.763	5.508	4.040	0.734	4.774	7.763
$Fe@C_{34}$	-2558.0444	-4.249	5.337	3.672	0.832	4.504	6.093
$Co@C_{34}$	-2677.1051	-3.290	5.500	4.074	0.713	4.787	8.035
Ni@C34	-2802.5968	-3.826	5.305	3.794	0.755	4.549	6.849
Cu@C34	-2934.7947	-2.529	5.479	3.754	0.862	4.616	6.177

Table 7. Thermodynamic properties at different temperatures at B3PW91/6-31G(d) level.

T(K)	H^0_m(kcalmol^{-1})		$C_p{}^0_m$(calmol^{-1}K^{-1})		S^0_m(calmol^{-1}K^{-1})	
	C_{34}	Ti-C_{34}	C_{34}	Ti-C_{34}	C_{34}	Ti-C_{34}
200	132.31	133.62	34.07	36.72	84.68	87.56
250	134.40	135.85	49.71	52.79	94.41	97.92
300	137.27	138.89	65.09	68.72	105.20	109.32
350	140.89	142.71	79.53	83.73	116.64	121.37
400	145.20	147.24	92.71	97.41	128.40	133.72
450	150.14	152.42	104.49	109.60	140.25	146.15
500	155.63	158.18	114.88	120.30	152.02	158.47
550	161.61	164.43	123.96	129.62	163.59	170.57
600	168.00	171.12	131.86	137.69	174.90	182.38

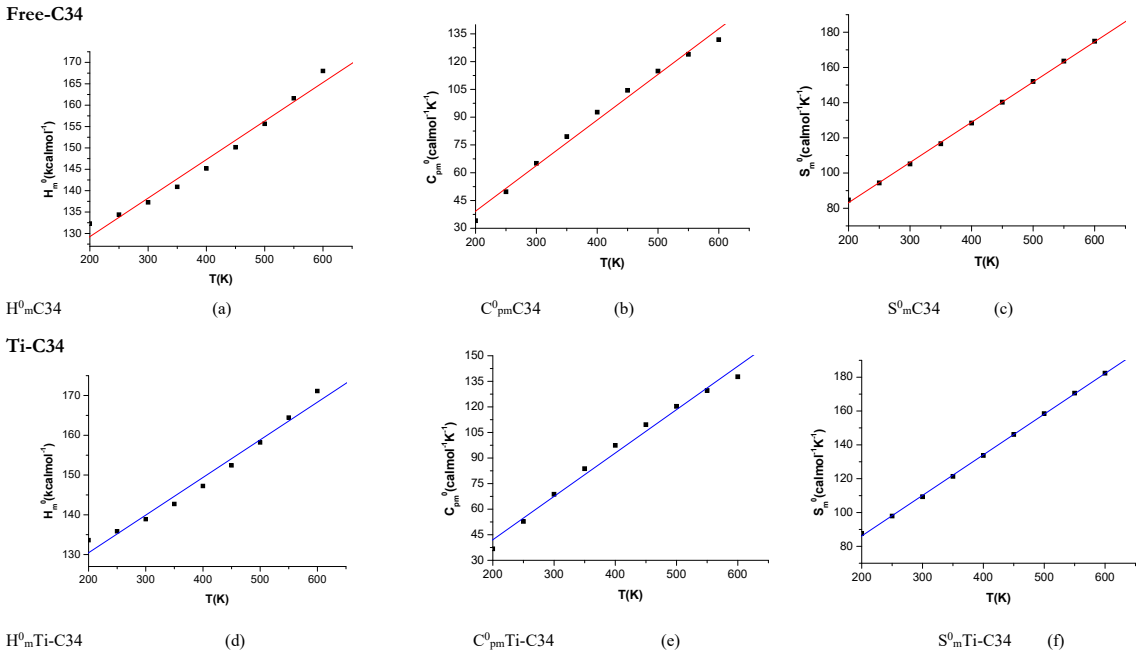

Fig. 7. Correlation graphics of thermodynamic properties and temperatures (a-f) for Free-"C_{34}" and Ti-"C_{34}".

Cu@C_{34} are situated in the center of ''C34'' cage. While Ti@C_{34}, V@C_{34}, Cr@C_{34}, Fe@C_{34}, Co@C_{34}, and Ni@C_{34} moved from the center towards one pentagonal face and then linked to this face. The cohesive energy of TM@C_{34} complexes suggests that Ti and V are most stable inside all cage structures, therefore indicating a strong possibility of their production. Cu is found to be least stable for encapsulation. All encapsulation processes are endothermic; this is likely due to swelling to the ''C34'' cage upon encapsulation of TM. Here, all eight TM@C34 is at the local minima because they have all real frequencies. The HOMO and LUMO of Mn@C34 and Cu@C34 indicates that there is no hybridization between the ''C34'' orbitals and the endohedral atom orbitals, while the HOMO and LUMO of Ti@C_{34}, V@C_{34}, Cr@C_{34}, Fe@C_{34}, Co@C_{34}, and Ni@C_{34} indicate that there exists hybridization between the ''C34'' orbitals and the end atom orbitals. It was also found that the energy gaps between HOMO and LUMO of TM@C_{34}(TM= Cr, and Co) are smaller than that of the empty ''C34'' cage. However, the energy gaps between HOMO and LUMO of TM@C_{34} (TM =Ti, V, Fe, Ni, and Cu) are larger than that of the empty ''C34'' cage. Natural population analysis shows that the charges always transfer from the TM atoms to the ''C34'' cage, so the fullerene ''C34'' cage acts an electron acceptor. In going from isolated TM atom to TM@C_{34}, the occupation of the 4s orbital is strongly reduced. The introduction to TM to the empty ''C34'' leads to more active NLO performance. The correlations between the thermodynamic properties $C^o_{p,m}$, S^o_m, H^o_m, and temperatures T are also obtained.

ACKNOWLEDGMENTS

This research was supported by the facilities of Dep. Chemistry, Faculty of Education, Ain Shams University. My gratitude and deep thanks to Prof. Dr. A.M. El Mahdy for his interests, and useful discussions.

CONFLICT OF INTEREST

The authors declare that there are no conflicts of interest regarding the publication of this manuscript.

REFERENCES

[1] Kroto H. W., Heath J. R., Brien S. C. O., Curl R. F., Smalley R. E., (1985), C60: Buckminsterfullerene. *Nature.* 318: 162-163.

[2] Akasaka T., Nagase S., Kluwer A., (2002), Handbook of carbon nano materials. *Academic Publisher Dordrecht the Netherlands.*

[3] Zhiyong W., Ryo K., Shinohara H., (2014), Metal-dependent stability of pristine and functionalized unconventional dimetallofullerene M2@Ih-C80. *J. Phys. Chem.* 118: 13953-13958.

[4] Watanabe S., Ishioka N. S., Sekine T., Kudo H., Shimomura H.,

Muramatsu H., Kume T., (2005), Conversion of endohedral 133Xe-fullerene to endohedral 133Xe-fullerenol to be used for nuclear medicine. *J. Radioanal Nucl Chem.* 266: 499-502.

[5] Chi M., Han P., Fang X., Jia W., Liu X., and Xu B., (2007), Density functional theory of polonium-doped endohedral fullerenes Po@C60. *J. Mo.l Struct. Theochem.* 807: 121-124.

[6] Shangfeng Y., Tao Wei., Fei J., (2017), When metal clusters meet carbon cages: Endohedral clusterfullerenes. *Chem. Soc. Rev.* 46: 5005-058.

[7] Kroto H. W., (1987), C60: Buckminsterfullerene: Some Inside Stories. *Nature*. 329: 529-531.

[8] Fowler P. W., Cremona J. E., Steer J. I., (1988), Physics and chemistry of the fullerenes. *Thear. Chim. Acta.* 73: 1-26.

[9] Schmalz T. G., Seitz W. A., Klein D. J., Hite G. E., (1988), Physics and chemistry of finite systems: From clusters to crystals. *J. Am. Chem. Soc.* 110: 1113-1127.

[10] Bakowies D., Thiel W., (1991), MNDO study of large carbon clusters. *J. Am. Chem. Soc.* 113: 3704-3714.

[11] Fowler P. W., Batten R. C., (1991), Fullerenes: Status and perspectives-proceedings of the first italian workshop. *J. Chem. Soc. Faraday Trans.* 87: 3103 -3104.

[12] Fowler P. W., (1991), Medicinal and bio-related applications. *J. Chem. Soc. Faraday Commun.* 87: 1945-1957.

[13] Zhendong Hu., Jian-Guo Dong., John R. Lombardi., Lindsay D. M., (1992), Optical and raman spectroscopy of mass-selected tungsten dimers in argon matrices. *J. Chem. Phys.* 97: 8811-8815.

[14] Enyashin A. N., Ivanovskaya V. V., Makurin Yu. N., Ivanovsk A. L., (2004), Modeling of the structure and electronic structure of condensed phases of small fullerenes C28 and Zn@C28. *Phys. Solid State.* 46: 1569-1573.

[15] Deng-Lu H., Rui-Bin Zh., Yan-Yan W., Cong-Mian Zh., Cheng-Fu P., Gui-De T., (2010), Room temperature ferromagnetism in Ni-doped ZnO films. *Curr. Appl. Phy.* 10: 124-128.

[16] Metrangolo P., Neukirch H., Pilati T., Resnati G., (2005), Halogen bonding based recognition processes: A world parallel to hydrogen bonding. *Theo.Chem.* 38: 386-395.

[17] Dorota B., Sanchez-Elsner T., Louafi F., Timothy M. M., Antonios G. K., (2011), Receptor-mediated interactions between colloidal gold nanoparticles and human umbilical vein endothelial cells. *Small.* 7: 388-391.

[18] Montero M. A., Gennero M. R., Chialvo D., Chialvo A. C., (2011), Electrocatalytic activity of core-shell Au@Pt nanoparticles for the hydrogen oxidation reaction. *Int. J. Hydrogen Energy.* 36: 3811-3816.

[19] Dhiman S., Kumar R., Dharamvir K., (2013), Structural and electronic properties of dilute magnetic oxides and Heusler Alloys. *Int. Conf. Recent Trend in Applied Physics and Material Science.* 1536: 847-897.

[20] Frisch M. J., Trucks G. W., Schlegel H. B.; Scuseria G. E., Robb M. A., Cheeseman J., Scalmani G., Barone V., Mennucci B. G. A., Petersson H., Nakatsuji M., Caricato X., Li H. P., Hratchian A. F., Izmaylov J., Bloino G., Zheng J. L., Sonnenberg M., Hada M., Ehara K., Toyota R., Fukuda J., Hasegawa M., Ishida T., Nakajima Y., Honda O., Kitao H., Nakai T., Vreven J. A., Montgomery Jr. J. E., Peralta F., Ogliaro M., Bearpark J. J., Heyd E., Brothers K. N., Kudin V. N., Staroverov T., Keith R., Kobayashi J., Normand K., Raghavachari A., Rendell J. C., Burant S. S., Iyengar J., Tomasi M., Cossi N., Rega J. M., Millam M., Klene J. E., Knox J. B., Cross V., Bakken C., Adamo J., Jaramillo R., Gomperts R. E., Stratmann O., Yazyev A. J., Austin R., Cammi C., Pomelli J. W., Ochterski R. L., Martin K., Morokuma V. G., Zakrzewski G. A., Voth P., Salvador J. J., Dannenberg S., Dapprich A. D., Daniels O., Farkas J. B., Foresman J. V., Ortiz J., Cioslowski and Fox D. J., Wallingford C. T., (2010), Inc., Gaussian.

[21] Becke A. D., (1993), Density-functional thermochemistry. III. The role of exact exchange. *J. Chem. Phys.* 98: 5648 -5652.

[22] Perdew J. P., Wang Y., (1992), Characterization of semiconductor heterostructures and nanostructures. *Phys. Rev.B.* 45: 13244-13249.

[23] Su K. H., Wei J., Hu X. L., Yue Lu H. L., (2000), Demonstration of high-resolution capability of chemical force titration via study of acid/base properties of a patterned self-assembled monolayer. *Acta Phys. Chem. Sin.* 16: 517-521.

[24] Su K. H., Wei J., Hu X. L., Yue Lu H. L., (2000), Size dependence of gas sensitivity of ZnO nanorods. *Acta Phys. Chem. Sin.* 16: 718-723.

[25] O'Boyle N. M., Tenderholt A. L., Langner K .M., Clib C., (2008), A library for package-independent computational chemistry algorithms. *J. Comput. Chem.* 29: 839-845.

[26] Fowler P W., Manolopoulos D. E., (1995), An atlas of fullerenes, clarendon oxford.

[27] Liu X., Schmalz T. G., Klein D. J., (1992), Favorable structures for higher fullerenes. *Chem. Phys. Lett.* 188: 550-554.

[28] Kessler B., Bringer A., Cramn S., Schlebusch C., Eberhardt W., Suzuki S., Achiba Y., Esch F., Barnaba M., Cocco D., (1997), Evidence for incomplete charge transfer and La-Derived states in the valence bands of endohedrally doped La@C82. *Phys. Rev. Lett.* 79: 2289-2292.

[29] Lu J., Zhang X., Zhao X., (2000), Metal-cage hybridization in endohedral La@C60, Y@C60 and Sc@C60. *Chem. Phys. Lett.* 332: 51-57.

[30] Wang K., Zhao J., Yang S., Chen L., Li Q., Wang B., Yang S., Yang J., Hou J G., Zhu Q., (2003), Unveiling metal-cage hybrid states in a single endohedral metallofullerene. *Phys. Rev. Lett.* 91: 185504-185508.

[31] Lu J., Mei W. N., Gao Y., Zeng X., Jing M., Li G., Sabirianov R., Gao Z., You L., Xu J., Yu D., Ye H., (2006), Structural and electronic properties of Gd@C60: All-electron relativistic total-energy study. *Chem. Phys. Lett.* 425: 82-84.

[32] Lu J., Zhang X., Zhao X., Nagase S., Kobayashi K., (2000), Strong metal-cage hybridization in endohedral La@C82, Y@C82 and Sc@C82. *Chem. Phys. Lett.* 332: 219-224.

[33] Manolopoulos D. E., May J. C., Down S. E., (1991), Theoretical studies of the fullerenes: C34 to C70. *Chem. Phys. Lett.* 181: 105-111.

[34] Andrew P. H., Thomas D. M., Timothy A.S., (2016), Structural biology and evolution of the TGF-β family. *J. Cold Spring Harb. Perspect. Biol.* 8: 22103-22109.

[35] Naray-Szabo G., Ferenczy G. G., (1995), Pharmacological aspects of molecular recognition. *Chem. Rev.* 95: 829-847.

[36] Shen Y. R., (1984), The principles of nonlinear optics, *John Wiley & Sons*, New York Wiley, NewYork.

[37] Prasad P. N., Williams D. J., (1990), Introduction to nonlinear optical effects in molecules and polymers. *Wiley New York.*

[38] Cinar M., Coruh A., Karabacak M., (2011), Spectroscopic (NMR, UV, FT-IR and FT-Raman) analysis and theoretical investigation of nicotinamide N-oxide with density functional theory. *Spectrochim. Acta. A.* 83: 250 -258.

[39] Chattaraj P. K., (1992), Analyzing the efficiency of Mn-(C_2H_4)

(M = Sc, Ti, Fe, Ni; n = 1, 2) complexes as effective hydrogen storage materials. *J. Indian. Chem. Soc.* 69: 173-183.

[40] Parr R. G., Donnelly R. A., Levy M., Palke W. E., (1978), Nanoscience and computational chemistry: Research progress. *J. Chem. Phys.* 68: 3801-3807.

[41] Parr R. G., Pearson R. G., (1983), Chemical modelling: Applications and theory. *J. Am. Chem. Soc.* 105: 7512 -7516.

[42] Pearson R. G., (1997), Chemical Hardness. *Wiley-VCH Weinheim.*

[43] Parr R. G., von L., Zentpaly S., Liu S., (1999), Electrophilicity index. *J. Am. Chem. Soc.* 121: 1922-1924.

[44] Chattaraj P. K., Sarkar U., Roy D. R., (2006), Perennial review. *Chem. Rev.* 106: 2065-2091.

[45] Chattaraj P. K., Roy D. R., (2007), Electrophilicity index. *Chem. Rev.*107: 46-74.

[46] Tanak H., (2014), Molecular structure, spectroscopic (FT-IR and UV-Vis) and DFT quantum-chemical studies on 2-[(2, 4-Dimethylphenyl) iminomethyl]-6-methylphenol. *Mol. Phys.* 112: 1553-1565.

[47] Tanak H., Marchewka M. K., Drozd M., (2013), Molecular structure and vibrational spectra of Bis(melaminium) terephthalate dihydrate: A DFT computational study. *Spectrochim. Acta A.* 105: 156-164.